K hindrance in primary γ decay after thermal and average resonance neutron capture

I. Huseby, T. S. Tveter, L. Bergholt, M. Guttormsen, E. Melby, J. Rekstad, and S. Siem
Department of Physics, University of Oslo, Box 1048 Blindern, N-0316 Oslo, Norway

R. K. Sheline
Departments of Chemistry and Physics, Florida State University, Tallahassee, Florida 32306
(Received 11 December 1996)

The intensities of primary γ-ray transitions following thermal and average resonance neutron capture have been found to display a dependence on the final-state K quantum number. The apparent K-hindrance effect is significantly stronger in the thermal than in the average resonance case. After thermal neutron capture, the intensity distributions indicate that the ''K-allowed'' transitions are associated with a higher number of degrees of freedom than the ''K-forbidden'' transitions. Possible explanations for the observed phenomena are discussed. [S0556-2813(97)04204-0]

PACS number(s): 23.20.Lv, 05.45.+b, 25.40.Lw, 27.70.+q

INTRODUCTION

The projection K of the total angular momentum on the symmetry axis has proved to be an interesting probe for the degree of chaos in rare earth nuclei. In a series of recent papers, evidence has been presented for an apparent K-hindrance effect in the primary γ decay of states populated through thermal and average resonance neutron capture in deformed nuclei [1–5]. This result has met considerable opposition, since the K quantum number is not expected to be conserved at so high excitation energy ($E_x \approx 6-8$ MeV), and alternative explanations have been presented [6–8].

It was pointed out by von Egidy [6] that the initial states are anisotropic with respect to K, even in the case of complete configuration mixing. A weak final-state K dependence arises naturally out of the K-dependent density of basis states. An interesting idea presented by Hansen [7] was that the apparent K hindrance may be due to an entrance-exit channel correlation effect, where resonances having large components with $K_i = K_{\text{target}} \pm 1/2$ in their wave function will be favored both in the neutron capture and in the subsequent ''allowed'' dipole γ decay. Barrett *et al.* [8] argued that the results of [1] were incompatible with the statistical model and, in particular, that the excellent agreement between Gaussian Orthogonal Ensemble (GOE) predictions and the nuclear data ensemble (NDE) for this mass region requires complete K mixing. This argument was found to be incorrect by Mottelson [9], since the NDE is a pure $I = K = 1/2$ ensemble and thus quite different from the resonance ensemble actually studied here (see next section).

The alternative interpretations listed above represent some very valuable ideas about the physics underlying the apparent K-hindrance effect found experimentally, but nevertheless fail to provide a comprehensive and satisfactory explanation of all aspects of the phenomenon.

EXPERIMENTAL DATA: ANALYSIS AND RESULTS

From the low energy regime, it is well known that a γ transition $K_i \rightarrow K_f$ is K forbidden if $\Delta K = |K_i - K_f| > \lambda$, where λ is the multipolarity of the radiation. The transition rate is then reduced by a factor of approximately $10^{2(\Delta K - \lambda)}$ [10].

Utilizing data available from the literature, we have studied the primary γ-ray transitions after thermal and average resonance (ARC) neutron capture, leading to the formation of the deformed nuclei ^{168}Er, ^{174}Yb, ^{178}Hf (even-even), ^{166}Ho, ^{176}Lu, ^{182}Ta (odd-odd), and ^{177}Lu (odd-Z), all with $K_{\text{target}} = 7/2$ except ^{174}Yb, which has $K_{\text{target}} = 5/2$. Tables of primary γ rays and level schemes are taken from Refs. [4,11–17].

Since s neutrons dominate completely at the low neutron energies used here, the capture states will have spin values $I_i = I_{\text{target}} \pm 1/2$ and parity π_{target}. The usual angular momentum coupling rules give $K_i = K_{\text{target}} \pm 1/2$ in the absence of K mixing. Final states with K values $K_{\text{target}} - 3/2 \leqslant K_f \leqslant K_{\text{target}} + 3/2$ can be reached through K-allowed dipole transitions, while transitions to states with $K_f = 0(1/2), \ldots, K_{\text{target}} - 5/2$ are forbidden.

The intensities of high energy primary dipole transitions from the neutron capture states to low-lying final states with known quantum numbers $I^{\pi}K$ have been investigated. Since the transition probabilities depend on the final-state spin and parity, transitions to levels within the same spin-parity groups only can be compared directly. It is desirable to be able to compare all transitions on the same scale, regardless of energy and multipolarity. Therefore, dimensionless relative reduced transition probabilities x_j into the various final states j have been extracted by dividing out the γ-energy dependence and the dependence on the final-state spin and parity [2]. The quantities x_j can then be grouped according to final-state K value and, eventually, into one ''forbidden'' and one ''allowed'' ensemble. A possible K dependence should then be revealed as different centroids and possibly different shapes for the x distributions obtained for forbidden and allowed transitions. An empirical ''hindrance factor'' has been defined as the ratio $R = \langle x \rangle_F / \langle x \rangle_A$, where $\langle x \rangle_F$ and $\langle x \rangle_A$ are the mean relative reduced transition probabilities of the forbidden and allowed transitions, respectively.

The earlier papers [1–5] concluded that there are apparent K-selection effects in the γ decay from the neutron reso-

TABLE I. Average reduced relative transition probabilities $\langle x\rangle_F$ and $\langle x\rangle_A$ for forbidden and allowed transitions, and effective hindrance factors $R=\langle x\rangle_F/\langle x\rangle_A$. The numbers of transitions in the various ensembles are listed in parentheses.

Nucleus	$\langle x\rangle_F$ (thermal)	$\langle x\rangle_A$ (thermal)	Ratio R (thermal)	$\langle x\rangle_F$ (2 keV)	$\langle x\rangle_A$ (2 keV)	Ratio R (2 keV)
^{168}Er	0.76 (18)	1.08 (48)	0.71	0.94 (17)	1.02 (30)	0.92
^{174}Yb	0.86 (7)	1.12 (8)	0.77	1.01 (7)	1.07 (8)	0.94
^{178}Hf	0.84 (15)	1.33 (9)	0.63	0.96 (14)	1.05 (10)	0.91
^{166}Ho	0.72 (17)	1.23 (21)	0.59	0.97 (19)	0.99 (26)	0.97
^{176}Lu	0.71 (17)	1.31 (16)	0.55	1.02 (17)	0.98 (13)	1.04
^{182}Ta	0.60 (7)	1.19 (15)	0.50	0.82 (6)	1.07 (11)	0.76
^{177}Lu	0.59 (10)	1.31 (13)	0.45			
All nuclei	0.73 (91)	1.19 (130)	0.62	0.96 (80)	1.02 (98)	0.94

nance region. Results for the individual nuclei are given in Table I. A striking observation is that the K hindrance seems more profound in thermal neutron capture than in ARC [2–5]. The hindrance factors R, averaged over all nuclei studied, are $R_{\rm therm}=0.62\pm0.11$ and $R_{\rm ARC}=0.94\pm0.09$. The uncertainties given here are calculated as the standard deviation of R for the ensemble of nuclei.

MODEL CALCULATIONS AND COMPARISONS WITH DATA

In order to explore the statistical behavior of allowed and forbidden transitions at different neutron energies, the observed transition probability distributions were compared with theoretical model calculations. The model constructed for simulating the neutron capture and subsequent γ decay is based on the following simple assumptions.

The capture states $\{i\}$ are described as linear combinations of basis configurations $\{j\}$ weighted by Porter-Thomas-distributed squared amplitudes $p_{i,j}$. The basis configurations considered show a direct correspondence with the set of final states in such a way that every initial configuration can decay to one distinct final state only, which for simplicity is referred to by the same index $\{j\}$. Each resonance is populated through one entrance component $j_{\rm entrance}$, the squared amplitude of which is drawn from the same Porter-Thomas distribution. The γ decay can then occur through any of the basis components into the corresponding final state j.

The probability Γ_j for transition to a given final state j from a total number n of populated resonances is given as a sum over the squared amplitudes $p_{i,j}$ of this configuration in the n populated initial states i, weighted by the entrance component squared amplitudes $p_{i,j_{\rm entrance}}$ of the respective states:

$$\Gamma_j=\sum_{i=1}^{n} p_{i,j}\cdot p_{i,j_{\rm entrance}}. \tag{1}$$

The reduced relative transition probabilities x_j are determined as $\langle x\rangle_{\rm expt}\Gamma_j/\langle\Gamma\rangle$. Here $\langle\Gamma\rangle$ is the average of all calculated Γ_j values, and $\langle x\rangle_{\rm expt}$ is the experimental average value for the ensemble considered, ensuring that the theoretical and experimental distributions have the same centroid.

The average resulting distribution of reduced relative transition probabilities x is simply a Porter-Thomas distribution (a χ^2 distribution with one degree of freedom) when one single resonance is populated. When n grows very large, it approaches a product distribution $\Sigma_{i=1}^{n}xy$, x and y being independent Porter-Thomas-distributed variables [18]. For finite n, the distribution displays a shape intermediate between a product distribution and a χ^2 distribution with n degrees of freedom.

Comparison of theoretical and experimental x distributions after thermal capture reveals an astonishing difference between K-allowed and K-forbidden transitions, as shown in Figs. 1(a) and 1(b). The allowed and forbidden distributions have both different centroids and shapes associated with different numbers n of initial states (degrees of freedom). The forbidden distribution displays both a large probability for very weak transitions and a long tail extending towards high x values, while the allowed distribution is more concentrated around its centroid. The allowed transitions roughly follow a distribution corresponding to $n_A\approx5$ initial states, while the distribution of forbidden transitions is well reproduced assuming $n_F\approx2$. The n value expected should be about 4 if the thermal neutrons hit between two different resonances for both available spin values $I_i=I_{\rm target}\pm1/2$, populating narrow intervals of their tail regions. In the immediate vicinity of one resonance, n would be somewhat smaller.

The experimental distributions from average resonance capture are well described assuming the same number of initial states, $n_A=n_F\approx110$, for both forbidden and allowed transitions [Figs. 1(c) and 1(d)]. This is about the number of populated resonances expected from the energy spread of the 2-keV neutron beam. It is interesting to note that the ratio n_A/n_F is about 2 for the thermal data, but close to unity at ARC energies.

The insets in Fig. 1 show the squared deviations between experimental and theoretical distributions as a function of n. The experimental uncertainties are taken to be the square roots of the numbers of transitions in the various histogram channels. The χ^2 minima are rather shallow, but the n values obtained agree well with qualitative expectations from visual inspection. To give an idea of the uncertainty in n, theoretical distributions for $n\pm1$ for thermal data and $n\pm20$ for ARC data are shown, as well as for n, plotted together with the data.

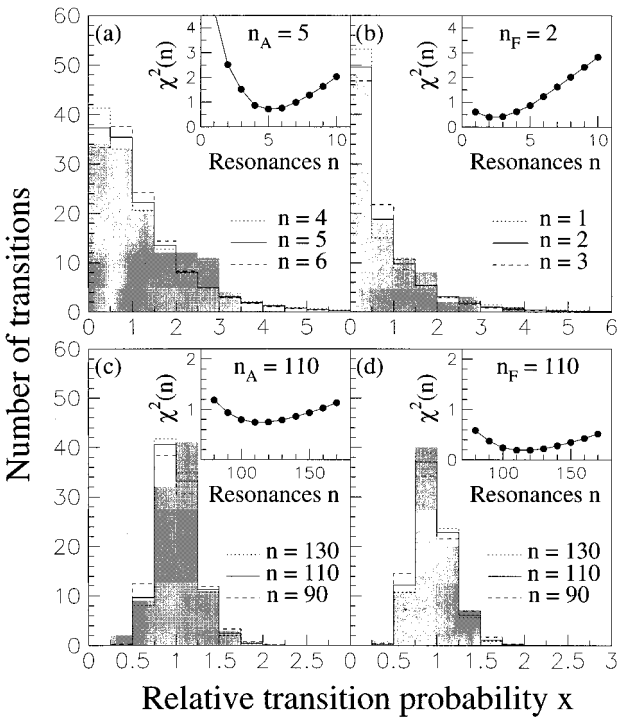

FIG. 1. Experimental distributions (solid histograms) of relative reduced transition probabilities x for (a) allowed and (b) forbidden transitions, thermal energies, and (c) allowed and (d) forbidden transitions, ARC energies. The data are compared with theoretical x distributions for different numbers n of resonances (open histograms). Insets: squared deviation χ^2 between calculated distributions and data for various n.

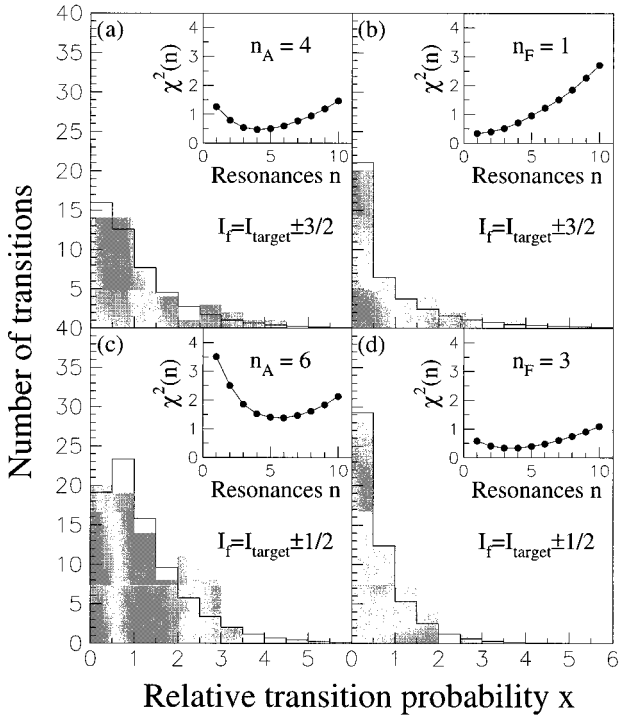

FIG. 2. Experimental x distributions for allowed and forbidden transitions after thermal neutron capture (solid histograms), separated into different spin groups, $I_f = I_{target} \pm 3/2$, for (a) allowed and (b) forbidden transitions, and $I_f = I_{target} \pm 1/2$, for (c) allowed and (d) forbidden transitions. The data are compared with theoretical x distributions for n resonances (open histograms). Insets: same as for Fig. 1.

To demonstrate that the observed pattern is unlikely to be an accidental consequence of limited statistics, we have split the transitions into four subsets according to their final-state spin, $I_f = I_{target} \pm 3/2$ and $I_f = I_{target} \pm 1/2$. The former group of transitions originates from only one of the two initial spin values possible ($I_i = I_{target} \pm 1/2$), while the latter may start from both of them. The split-ensemble experimental data, compared with theoretical calculations, are displayed in Fig. 2 (see caption for details). Best fits to the various subensembles are obtained with the following numbers n of resonances: $I_f = I_{target} \pm 3/2$, $n_A \approx 4$, $n_F \approx 1$; $I_f = I_{target} \pm 1/2$, $n_A \approx 6$, $n_F \approx 3$. The allowed-forbidden difference is obvious in all the individual subsets investigated. It is also interesting to note that the distributions associated with $I_f = I_{target} \pm 1/2$ correspond to approximately twice as many initial states as the $I_f = I_{target} \pm 3/2$ distributions, as expected. This observation inspires confidence in the statistical quality of the data and the possibility of extracting physically relevant information from the distribution shapes.

DISCUSSION

A satisfactory theory has to explain the striking difference between the probability distributions for K-allowed and K-forbidden transitions, both with respect to centroids and shapes, seen in the thermal, but not in the ARC data. The two groups of resonance states, separated in energy by only 2 keV, are expected to be equivalent with respect to quantal structure, with the same degree of configuration mixing. The observed difference between the two neutron energies remains a mystery so far, but a few simple speculations about the underlying physics are presented below.

One possible explanation for the difference between n_F and n_A could be K mixing for a subset of the neutron resonances. In that case, the ''K-allowed'' final states can be reached through allowed transitions from all populated states, while the ''K-forbidden'' ones are only accessible from the K-mixed initial states. A problem with this explanation is that a model assuming two classes of resonance wave functions with different degrees of K mixing is not consistent with the observation that $n_A \approx n_F$ for the ARC data.

Alternatively, the extra degrees of freedom might be associated with the decay instead of the population process. The question is then why the additional exit components, exclusive to the allowed decay, vanish in the ARC case. One obvious difference between the resonances populated at the two energies is their neutron width. Since neutron emission mainly occurs through the high-K entrance component with an s neutron located in continuum, this configuration and related ones are expected to contribute less to the γ decay at $E_n = 2$ keV. The mathematical consequences of such an entrance-exit correlation, which goes beyond our simple model of decay through randomly chosen exit components, need to be studied in greater detail.

An intriguing question is whether there might be fundamental structural differences between the states populated by

thermal and ARC neutrons. The ARC neutrons, which have an energy spread of several hundreds of eV, will populate $\sim 10^2$ resonance states, and the resulting x distributions will mainly show the properties of the resonances themselves. At thermal energies, the resonance states display an average width ~ 1 eV and spacing ~ 10 eV for a given spin value. The thermal neutrons enter the nuclei at $E_n \approx B_n + 1/30$ eV with a very small energy spread and are most likely to hit between two resonances, populating a narrow interval of their tail regions. The associated transition probability distributions will reflect the quantal properties of the resonance tails and possibly additional background. One may speculate whether the thermal cross section includes some kind of nonresonant states with less K mixing than the resonances dominating the ARC cross section. It is not clear how such states should be modeled mathematically. One possible contribution to the nonresonant cross section might be potential capture, where γ decay takes place directly from the entrance component [19].

The main objective of this paper has been to present the experimental results and to point at possible interpretations in a qualitative and nonexhaustive way. To advance from this point, we plan an empirical study of correlations between transition probability and final-state microscopic structure, for instance, in terms of the similarity to the entrance configuration, as initiated by Soloviev [20]. More sophisticated simulations, encompassing possible entrance-exit correlation effects and single-particle selection rules, are needed. Experimental studies aimed at understanding the capture, thermalization, and decay processes and the quantal structure of the narrow resonances and the continuum between them would be of great value.

SUMMARY AND CONCLUSIONS

The primary γ decay of an ensemble of well-deformed nuclei after thermal and 2-keV neutron capture reveals a significant difference in the average transition probabilities for K-allowed and K-forbidden transitions. The effect is considerably stronger at thermal energies, where the effective hindrance factor $R = \langle x \rangle_F / \langle x \rangle_A$ equals 0.62 ± 0.11, compared to 0.94 ± 0.09 in the ARC data. This seems to indicate a smaller degree of K mixing among the states populated by thermal neutron capture, which is quite surprising.

Simulations of the neutron capture and the subsequent γ decay have been performed in a schematic model with Porter-Thomas-distributed basis configurations. The number of degrees of freedom needed to reproduce the shape of the transition probability distributions measured after thermal neutron capture is approximately twice as large for K-allowed as for K-forbidden transitions. This suggests that the higher average intensity of K-allowed transitions may be due to a higher number of contributions. In the ARC data, the same number of degrees of freedom (~ 110) describes the distribution shapes regardless of K forbiddenness.

The physical interpretation of these results is still uncertain. One possibility is that the allowed transitions after thermal capture originate from a higher number of initial states, including continuum states between the resonances. Alternatively, the number of available initial states may be the same for all transitions, but the allowed decay may take place through a higher number of exit components. Since the γ-decay pattern after thermal neutron capture seems to indicate less K mixing than in the ARC case, one may speculate whether the thermal neutrons populate states with less K mixing than the ordinary resonance states.

Further experimental and theoretical studies are necessary in order to shed light on the physical mechanisms responsible for the observed effects.

ACKNOWLEDGMENTS

Financial support from the Norwegian Research Council (NFR) and from Florida State University (NSF Contract No. PHY 92-07336) is gratefully acknowledged. Inspiring discussions with T. Døssing and T. L. Khoo are greatly appreciated.

[1] J. Rekstad, T. S. Tveter, and M. Guttormsen, Phys. Rev. Lett. **65**, 2122 (1990).

[2] J. Rekstad, T. S. Tveter, M. Guttormsen, and L. Bergholt, Phys. Rev. C **47**, 2621 (1993).

[3] L. Bergholt, M. Guttormsen, J. Rekstad, T. S. Tveter, and R. K. Sheline, Phys. Rev. C **50**, 493 (1994).

[4] R. K. Sheline, L. Bergholt, M. Guttormsen, J. Rekstad, and T. S. Tveter, Phys. Rev. C **51**, 3078 (1995).

[5] T. S. Tveter, L. Bergholt, J. Rekstad, M. Guttormsen, and R. K. Sheline, Acta Phys. Pol. B **26**, 383 (1995).

[6] T. von Egidy, in *Nuclear Shapes and Nuclear Structure at Low Excitation Energies*, Proceedings of a NATO Advanced Research Workshop, Cargese, France, 1991, edited by M. Vergnes *et al.* (Plenum, New York, 1993), p. 373.

[7] P. G. Hansen, Phys. Rev. Lett. **67**, 2235 (1991).

[8] B. R. Barrett, R. F. Casten, J. N. Ginocchio, T. Seligman, and H. A. Weidenmüller, Phys. Rev. C **45**, R1417 (1992).

[9] B. R. Mottelson, in *Proceedings of the International Seminar on the Frontier of Nuclear Spectroscopy*, Kyoto, Japan, 1992 (Singapore, World Scientific, 1993), p. 7.

[10] Aa. Bohr and B. R. Mottelson, *Nuclear Structure* (Benjamin, New York, 1976), Vol. 2, p. 155.

[11] W. F. Davidson, D. D. Warner, R. F. Casten, K. Schreckenbach, H. G. Börner, J. Simic, M. Stojanovic, M. Bogdanovic, S. Koicki, W. Gelletly, G. B. Orr, and M. L. Stelts, J. Phys. G **7**, 455 (1981); W. F. Davidson, W. R. Dixon, and R. S. Storey, Can. J. Phys. **62**, 1538 (1984); W. F. Davidson and W. R. Dixon, J. Phys. G **17**, 1683 (1991).

[12] W. Gelletly, J. R. Larysz, H. G. Börner, R. F. Casten, W. F. Davidson, W. Mampe, K. Schreckenbach, and D. D. Warner, J. Phys. G **13**, 69 (1987); R. C. Greenwood and C. W. Reich, Phys. Rev. C **23**, 153 (1981).

[13] A. M. I. Hague, R. F. Casten, I. Forster, A. Gelberg, R. Rascher, R. Richter, P. von Brentano, G. Berreau, H. G. Börner, S. A. Kerr, K. Schreckenbach, and D. D. Warner, Nucl. Phys.

A455, 231 (1986); E. P. Grigor'ev, Phys. At. Nucl. **58**, 523 (1995).

[14] T. J. Kennett, M. A. Islam, and W. W. Prestwich, Phys. Rev. C **30**, 1840 (1984); L. M. Bollinger and G. E. Thomas, *ibid.* **2**, 1951 (1970); E. Shurshikov and N. V. Timofeeva, Nucl. Data Sheets **67**, 45 (1992); M. K. Balodis, J. Berzins, V. Bondarenko, P. Prokofjevs, and A. V. Afanasjev, in *Proceedings of the 8th International Symposium on Capture Gamma-Ray Spectroscopy and Related Topics*, Fribourg, Switzerland, 1993, edited by J. Kern (Singapore, World Scientific, 1994), p. 268.

[15] M. M. Minor, R. K. Sheline, E. B. Shera, and E. T. Jurney, Phys. Rev. **187**, 1516 (1969); A. Fubini, D. Prosperi, F. Terrasi, and I. Vata, Nuovo Cimento A **8**, 748 (1972); R. W. Hoff, R. F. Casten, M. Bergoffen, and D. D. Warner, Nucl. Phys. **A437**, 285 (1985); N. Klay, F. Käppeler, H. Beer, G. Schatz, H. Börner, F. Hoyler, S. J. Robinson, K. Schreckenbach, B. Krusche, U. Mayerhofer, G. Hlawatsch, H. Lindner, T. von Egidy, W. Andrejtscheff, and P. Petkov, Phys. Rev. C **44**, 2801 (1991).

[16] R. G. Helmer, R. C. Greenwood, and C. W. Reich, Nucl. Phys. **A168**, 449 (1971); R. B. Firestone, Nucl. Data Sheets **54**, 307 (1988).

[17] B. Michaud, J. Kern, L. Ribordy, and L. A. Schaller, Helv. Phys. Acta **45**, 93 (1972).

[18] P. G. Hansen, B. Jonson, and A. Richter, Nucl. Phys. **A518**, 13 (1990).

[19] A. M. Lane and J. E. Lynn, Nucl. Phys. **17**, 563 (1960); **17**, 586 (1960).

[20] V. G. Soloviev, Phys. Lett. B **317**, 501 (1993).